A Printed Dual-band Coupler Using Modified Generalized Negative-Refractive-Index Transmission Lines

Colan G.M. Ryan, Student Member, IEEE and George V. Eleftheriades, Fellow, IEEE

The Edward S. Rogers, Sr. Dept. of Electrical and Computer Engineering
University of Toronto, Toronto, ON, M5S 3G4, Canada

***Abstract* — A dual-band printed metamaterial coupler made of a microstrip line and a generalized negative-refractive index line is presented. Due to the presence of two left-handed bands in the unit cell, backward coupling occurs over two frequency ranges centered on 2.7 GHz and 4.7 GHz. Measured results for an edge-coupled device are reported.**

***Index Terms* — Coupler, metamaterial, generalized negative-refractive-index transmission-line.**

I. INTRODUCTION

Practical implementations of metamaterials in the microwave band have primarily focused on loading regular microstrip (MS) lines with series capacitors and shunt inductors to form negative-refractive-index transmission lines (NRI-TLs) and with this technique many novel devices with interesting properties have emerged. Pertinent to this work is the microstrip/negative-refractive-index transmission line coupler reported in [1]. In a further analysis in [2], it was shown that backward coupling in this device occurs at the frequency where the dispersion curves of the isolated microstrip line and of the left-handed propagation band of the NRI transmission line intersect. About this point, a coupled-mode stopband is formed featuring two eigenmodes with complex-conjugate propagation constants leading to oppositely directed power flows on each line. An interesting property reported in [1] was the higher coupling level possible in the MS/NRI-TL coupler compared to traditional microstrip edge couplers of similar dimensions; also, in [3], it was observed that one of the modes in the stopband exhibits negative group velocity despite the coupler being formed from a lossless circuit. Here, we use generalized NRI-TLs to present a fully-printed dual-band MS/NRI-TL coupler. This generalized NRI-TL was introduced in [4] with its salient feature of two pairs of right-and left-handed propagation bands arising from the inclusion of four resonators in the equivalent circuit as opposed to two in the standard NRI-TL. By appropriately choosing the equivalent circuit parameters of the unit cell, the location of its two left-handed bands can be specified, as consequently can the two resulting coupling frequency bands. In this paper, we present the design of and results for an edge-coupled printed structure.

This paper is organized as follows. Section 2 gives an overview of the generalized NRI-TL cell and describes its fully-printed implementation. Section 3 discusses the analysis of the coupler unit cell and presents the simulated results. Measured results are reported in Section 4, while conclusions and remarks are made in Section 5.

II. UNIT-CELL DESIGN

The circuit diagram of the unit cell used in the NRI-TL section of the coupler is shown in Fig. 1. Derived from the pi-model of a regular NRI-TL equivalent circuit, this unit cell is a modification of the T-model cell presented in [4], but still possesses two pairs of right- and left-handed propagation bands. The advantage of this layout is its single C_{HP}/L_{HP} resonator which reduces fabrication complexity. Additionally, the C_{HS}/L_{HS} resonator is moved to the cell terminations to accommodate the length of transmission line that synthesizes both the C_{HP} and C_{HS} capacitances.

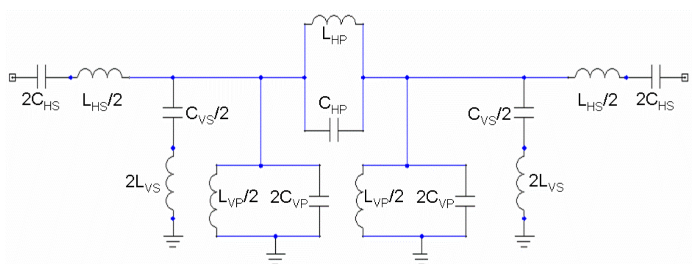

Fig. 1. Equivalent circuit for a modified generalized negative-refractive-index transmission-line unit cell.

An illustration of the fully-printed cell is given in Fig. 2 with the corresponding circuit elements labeled. The capacitances C_{HS} and C_{HP} are synthesized by parallel plates which yield a constant capacitance over a larger bandwidth than would an interdigitated capacitor. As shown in the figure, these parallel plates overlap on one side of the trace only; on the other side, they are directly connected to the main line by vias through the substrate. Table I lists the desired circuit values and the required dimensions of the printed cell.

TABLE I
SUMMARY OF CIRCUIT PARAMETERS AND PRINTED CELL DIMENSIONS

Circuit Values		Printed Cell Dimensions	
C_{HS}	0.455 pF	C_{HS} Overlap	0.8 mm
L_{HS}	5.47 nH	C_{HP} Overlap	0.4 mm
C_{HP}	0.928 pF	L_{HP} Gap	1.4 mm
L_{HP}	2.23 nH	L_{HP} Trace Width	0.2 mm
C_{VS}	0.932 pF	C_{VS} Width	3 mm
L_{VS}	2.32 nH	C_{VS} Length	3.5 mm
C_{VP}	0.455 pF	L_{VP} Length	2.3 mm
L_{VP}	0.910 nH	L_{VP} Width	0.3 mm
		L_{VS} Length	9 mm
		L_{VS} Width	0.3 mm
		Trace Width	5.2 mm
		Cell Length	14 mm

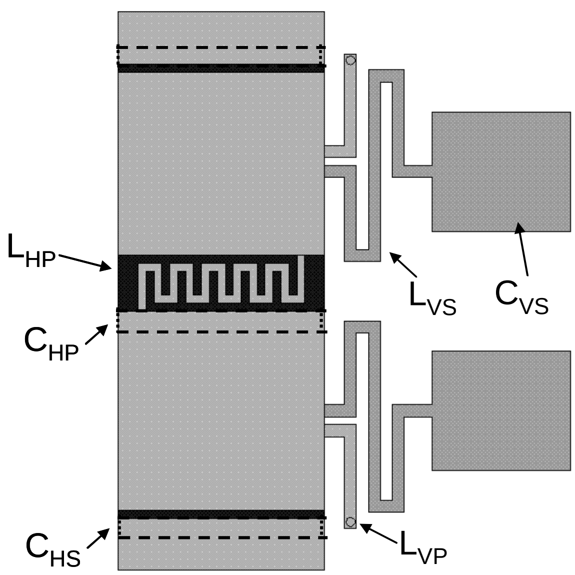

Fig. 2. Implementation of a generalized NRI-TL circuit as a fully-printed unit cell for an edge coupler. Dotted lines show areas of overlap for the parallel plate capacitors and solid black areas denote underlying parallel plates.

III. SIMULATED RESULTS

A. Unit Cell Dispersion

Using coupled-mode theory presented in [5], the propagation constants for the microstrip/generalized NRI coupler can be determined. In such a device, the propagation constants (γ) for the coupler's two eigenmodes can be determined according to the following equations:

$$\gamma^2 = \frac{1}{2}(a_1 + a_2) \pm \frac{1}{2}\sqrt{(a_1 - a_2)^2 + 4b_1 b_2}$$
$$a_1 = Y_1 Z_1 + Y_m Z_m, a_2 = Y_2 Z_2 + Y_m Z_m \quad . \quad (1)$$
$$b_1 = Y_m Z_1 + Y_2 Z_m, b_2 = Y_m Z_2 + Y_1 Z_m$$

Z_1, Y_1 and Z_2, Y_2 represent the per-unit-length impedance and admittance of the microstrip and NRI lines, respectively, while Z_m and Y_m account for the inductive and capacitive coupling between the lines. For the generalized NRI-TL circuit of Fig. 1, the impedance and admittance expressions are given as

$$Z_1 = j\omega L_0, Y_1 = j\omega C_0$$
$$Z_m = j\omega L_m, Y_m = -j\omega C_m$$
$$Z_2 = j\omega L_{HS} + \frac{1}{j\omega C_{HS}} + (j\omega C_{HP} + \frac{1}{j\omega L_{HP}})^{-1}$$
$$Y_2 = j\omega C_{VP} + \frac{1}{j\omega L_{VP}} + (j\omega L_{VS} + \frac{1}{j\omega C_{VS}})^{-1} \quad . \quad (2)$$

where L_0 and C_0 are the per-unit length inductance and capacitance of the microstrip line. After computing the mutual capacitance and inductance between the lines from [6], the dispersion diagram of the coupler unit cell was determined and is plotted in Fig. 3; Ansoft HFSS' Eigenmode solver [7] was used to verify these results for the printed structure and it is seen that good agreement between the two methods is obtained. The graph shows the expected band splitting where the microstrip mode dispersion curve intersects the left-handed band of the generalized NRI-TL cell, and therefore, backward-wave coupling is anticipated between approximately 2.4 GHz to 2.6 GHz and 4.1 GHz to 4.5 GHz.

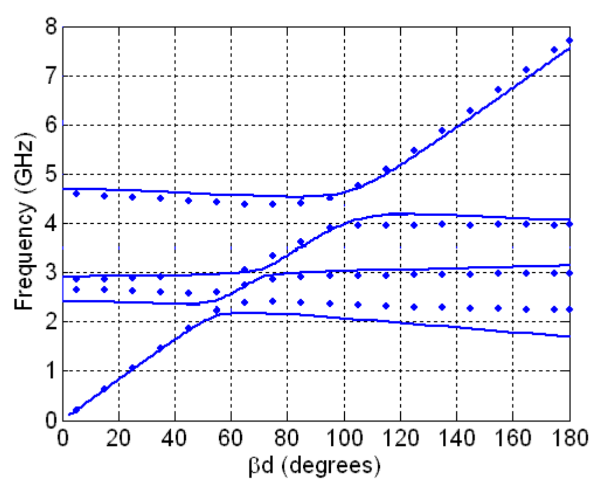

Fig. 3. Dispersion diagram from analytical solution (solid line) and HFSS full-wave simulation (dots).

B. Simulated Coupler Performance

HFSS was used to analyze the 3-cell coupler. Perfect conductors were assumed but substrate dielectric losses were included in the simulation; all ports were terminated with 50 Ω loads. Fig. 4 and Fig. 5 show the simulated S-parameters as well as the insertion loss (*IL*) calculated from

$$IL = -10\log(|S_{11}|^2 + |S_{21}|^2 + |S_{31}|^2 + |S_{41}|^2). \quad (3)$$

The coupling frequencies are well predicted by the analytical and eigenmode solution methods. The peak coupling magnitude at the lower and upper bands is -3.5 dB and -2.2 dB, respectively, while the return loss and isolation reach approximately -20 dB. The insertion loss is also negligible: it is less than 0.2 dB over the lower coupling band and less than 0.5 dB over the upper band.

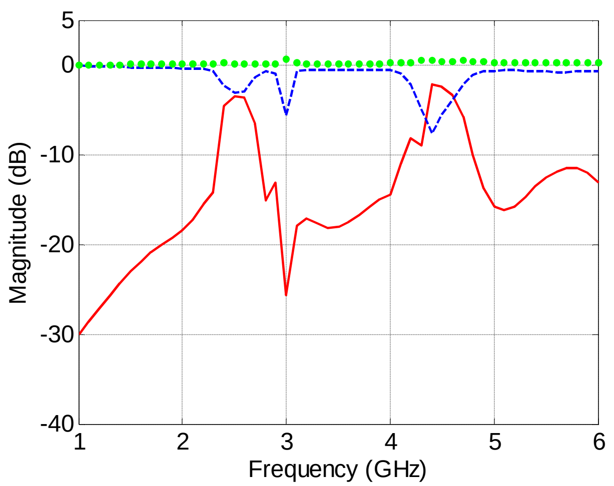

Fig. 4. Simulated S-parameters for 3-cell edge coupler showing magnitude for coupled (▬▬), through (▪ ▪ ▪), and calculated insertion loss (⋯⋯).

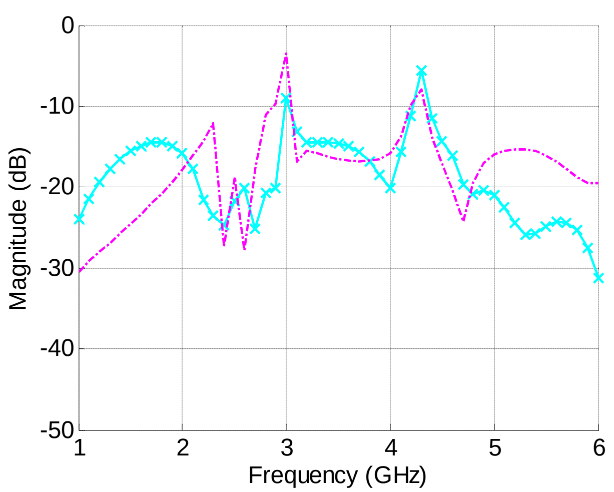

Fig. 5. Simulated S-parameters for 3-cell edge coupler showing magnitude for reflection (✕✕✕) and isolation (▬ ▪ ▬ ▪).

IV. MEASURED RESULTS

The fabricated coupler is pictured in Fig. 6. It is manufactured on a Rogers RT/Duroid 5880 substrate (ε_r=2.2) with a 0.127 mm top layer and a 1.524 mm bottom layer. Measured results are given in Fig. 7 and Fig. 8 and the coupler shows good agreement with the theoretical performance simulated in HFSS. Peak coupling levels of -3.5 dB and -4.4 dB are observed at 2.7 GHz and 4.7 GHz, respectively. The return loss is better than -20 dB and the isolation over the two coupling bands is also better than 20 dB.

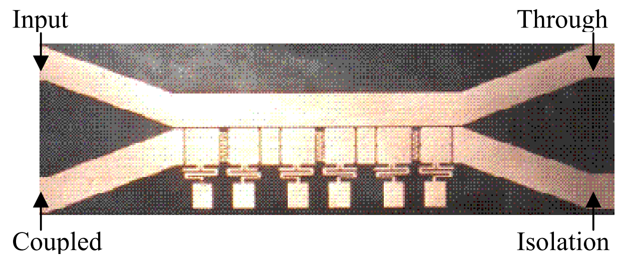

Fig. 6. Photographs of fabricated edge coupler with port conventions labeled. The NRI-TL line is 5.2 mm wide and the microstrip line is 4.8 mm wide. Including the feed lines, the overall dimensions are width= 30 mm, length= 90 mm.

The calculated insertion loss for this coupler over the lower band (2.6 GHz to 2.9 GHz) is typically below 1 dB and reaches 1.4 dB at the band edge; over the upper band from 4.65 GHz to 4.95 GHz, the maximum loss is 1.9 dB but is also typically around 1 dB. As verified with HFSS, the upward shift in coupling band frequencies as compared to the simulated results is partly due to the inclusion of the angled transmission-line feeding segments, as shown in Fig. 6. The drop in coupling magnitude of 2.2 dB at the upper band may be attributed to air gaps between the top and bottom layers which could not be completely eliminated and were not accounted for in the simulation. Furthermore, the length of the shorted stubs was slightly increased as the vias were soldered in place, thus contributing small errors in the final fabricated version. A comparison of the measured and simulated results is given in Table 2.

TABLE II

SUMMARY OF MEASURED AND SIMULATED RESULTS

Parameter	Simulated	Measured
Coupling Bands (GHz)	2.4-2.7/4.4-4.7	2.6-2.9/4.65-4.95
Max. Coupling (dB)	-3.5/-2.2	-3.5/-4.4
Min. Return Loss (dB)	-25.17/-19.6	-21.9/-30.6
Min. Isolation (dB)	-27.9/-24.3	-23.2/-21.6
Typical Insertion Loss (dB)	0.2/0.5	1.0/1.0

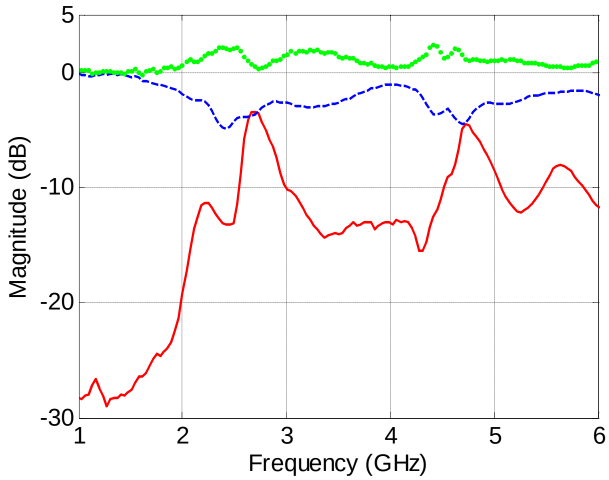

Fig. 7. Measured S-parameters for 3-cell edge coupler showing magnitude for coupled (▬), through (▪▪▪), and calculated insertion loss (▪▪▪▪▪▪).

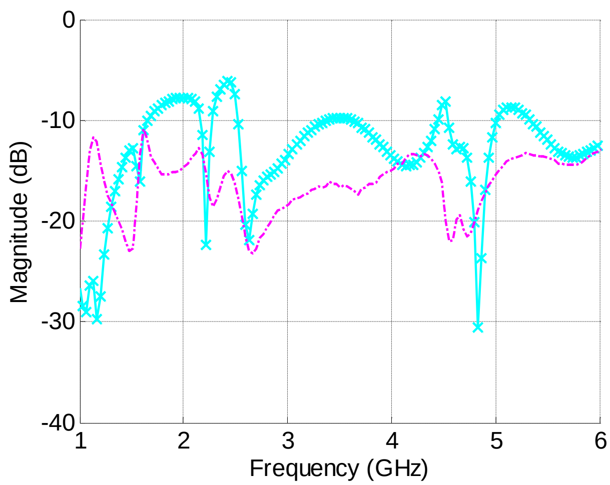

Fig. 8. Measured S-parameters for 3-cell edge coupler showing magnitude for reflection (✱✱✱) and isolation (▬ ▪ ▬ ▪).

V. CONCLUSION

A dual-band microstrip/NRI-TL metamaterial coupler using a fully-printed geometry has been designed, fabricated, and tested. Good performance has been obtained and deviations from the theoretical results have been discussed. Peak coupling levels of -3.5 dB and -4.4 dB were measured at 2.7 GHz and 4.7 GHz while maintaining the return loss and isolation under -20 dB and the insertion loss to approximately 1 dB over the two bands. Measured results testify to the sensitivity of this device to fabrication errors and suggest a strategy for reducing this sensitivity. For example, all elements could be printed on a single layer which would eliminate air gaps and simplify the fabrication process. Nevertheless, the present implementation features good dual-band performance.

REFERENCES

[1] R. Islam and G.V. Eleftheriades, "A planar metamaterial co-directional coupler that couples power backwards," *2003 IEEE MTT-S Int. Microwave Symp. Dig.,* vol. 1, pp. 321-324, June 2003.

[2] R. Islam, F. Elek, and G.V. Eleftheriades, "Coupled-line metamaterial coupler having co-directional phase but contra-directional power flow," *IEE Electronics Letters*, vol. 50, no. 5, pp. 315-317, March 2004.

[3] H. Mirzaei and G.V. Eleftheriades, "Negative and zero group velocity in microstrip/negative-refractive-index transmission line couplers," *2010 IEEE MTT-S Int. Microwave Symp. Dig.*, pp. 37-40, May 2010.

[4] G.V. Eleftheriades, "A generalized negative-refractive-index transmission-line (NRI-TL) metamaterial for dual-band and quad-band applications", *IEEE Microw. Wireless Compon. Lett.*, vol 17, no. 6, pp 415-417, June 2007.

[5] K.C. Gupta, I.J. Bahl, P. Bhartia, and R. Garg, *Microstrip Lines and Slotlines*, Artech House Inc., 1996.

[6] S.S. Bedair, "Characteristics of some asymmetrical coupled transmission lines", *IEEE Trans. Microwave Theory & Tech.,* vol. 32, no. 1, pp. 108-110, January 1984.

[7] Online. Available: http://www.ansoft.com, Ansoft HFSS, The 3D, electromagnetic, finite-element simulation tool for high-frequency design.